

# Saccades From Torsional Offset Positions Back to Listing's Plane

CHOONGKIL LEE,<sup>1</sup> DAVID S. ZEE,<sup>2</sup> AND DOMINIK STRAUMANN<sup>3</sup>

<sup>1</sup>Department of Psychology, Seoul National University, Seoul 151-742, Korea; <sup>2</sup>Department of Neurology, Johns Hopkins University, Baltimore, Maryland 21287; and <sup>3</sup>Department of Neurology, Zurich University Hospital, CH-8091 Zurich, Switzerland

**Lee, Choongkil, David S. Zee, and Dominik Straumann.** Saccades from torsional offset positions back to Listing's plane. *J Neurophysiol* 83: 3241–3253, 2000. Rapid eye movements include saccades and quick phases of nystagmus and may have components around all three axes of ocular rotation: horizontal, vertical, and torsional. In this study, we recorded horizontal, vertical, and torsional eye movements in normal subjects with their heads upright and stationary. We asked how the eyes are brought back to Listing's plane after they are displaced from it. We found that torsional offsets, induced with a rotating optokinetic disk oriented perpendicular to the subject's straight ahead, were corrected during both horizontal and vertical voluntary saccades. Thus three-dimensional errors are synchronously reduced during saccades. The speed of the torsional correction was much faster than could be accounted for by passive mechanical forces. During vertical saccades, the peak torsional velocity decreased and the time of peak torsional velocity was delayed, as the amplitude of vertical saccades increased. In contrast, there was no consistent reduction of torsional velocity or change in time of peak torsional velocity with an increase in the amplitude of horizontal saccades. These findings suggest that 1) the correction of stimulus-induced torsion is neurally commanded and 2) there is cross-coupling between the torsional and vertical but not between the torsional and horizontal saccade generating systems. This latter dichotomy may reflect the fact that vertical and torsional rapid eye movements are generated by common premotor circuits located in the rostral interstitial nucleus of the medial longitudinal fasciculus (riMLF). When horizontal or vertical saccade duration was relatively short, the torsional offset was not completely corrected during the primary saccade, indicating that although the saccade itself is three-dimensional, saccade duration is determined by the error in the horizontal or the vertical, but not by the error in the torsional component.

## INTRODUCTION

The brain stem saccade generators produce rapid eye movements, including quick phases, that rotate the globe around all three axes: horizontal, vertical, and torsional. The paramedian reticular formation in the pons (PPRF) encodes signals for the horizontal component of saccades, and the rostral interstitial nucleus of the medial longitudinal fasciculus (riMLF) in the midbrain encodes signals for the vertical and torsional components of saccades. Voluntary control of torsional rapid eye movements is limited, however; torsional quick phases do occur during vestibular stimulation but only a rare subject can make voluntary torsional saccades (Balliet and Nakayama 1978). Nevertheless, several investigators have suggested that the oculomotor system takes three-dimensional eye orientation

into account when generating voluntary saccades (Klier and Crawford 1998; Tweed et al. 1998). Van Opstal et al. (1996) also suggested that there is active neural control of torsion associated with saccades; electrical stimulation in the nucleus reticularis tegmenti pontis (NRTP) perturbed the torsional orientation of the eye, which was corrected in association with the next horizontal or vertical saccade. Lesions in this same area interfered with corrections of torsional offsets.

Although three-dimensional eye orientation appears to be neurally commanded, any torsional movement during horizontal or vertical saccades with head stationary is normally minimized as dictated by Listing's law, except for a small torsional transient, or "blip", up to 1–2° (Bruno and Van den Berg 1997; Straumann et al. 1995, 1996; Tweed et al. 1994). Listing's law states that the three-dimensional orientation of all rotation axes that bring the eyes from the reference position to an eccentric position lie in a single plane that is roughly perpendicular to the straight ahead eye position (Helmholtz 1867). Listing's law is a specification of Donders' law, which states that for every eccentric eye position there is a specific torsional orientation of the eye (Donders 1848). It is Listing's law that formulates the mathematical relation between the torsional orientation of the eye and the horizontal-vertical direction of gaze and quantitatively specifies "desired" torsional orientation. The rationale of Listing's or Donders' laws is not firmly established; no single motor or sensory hypotheses is completely satisfactory (Hepp et al. 1997; Melis and van Gisbergen 1995; Tweed et al. 1998).

In this study, we used roll optokinetic stimulation, around the line of sight of subjects with their heads upright and stationary, to produce torsional errors that drove the eyes out of Listing's plane. We asked how such torsional errors were corrected during subsequent horizontal and vertical saccades. We specifically investigated the dynamic properties of the movements that corrected such torsional errors (and brought the eyes back to Listing's plane) and how the torsional corrections interacted with the horizontal and vertical components of voluntary saccades.

## METHODS

### Subjects

Four normal male subjects (*CL*, *DZ*, *MH*, and *NH*, 21–52 yr of age) participated in this study. The nature and possible consequences of the experiments were explained to each subject, and informed consent, approved by The Johns Hopkins University Committee on Clinical Investigation, was obtained. The subjects had no prior history of ocular motility disorders and were taking no medications.

The costs of publication of this article were defrayed in part by the payment of page charges. The article must therefore be hereby marked "advertisement" in accordance with 18 U.S.C. Section 1734 solely to indicate this fact.

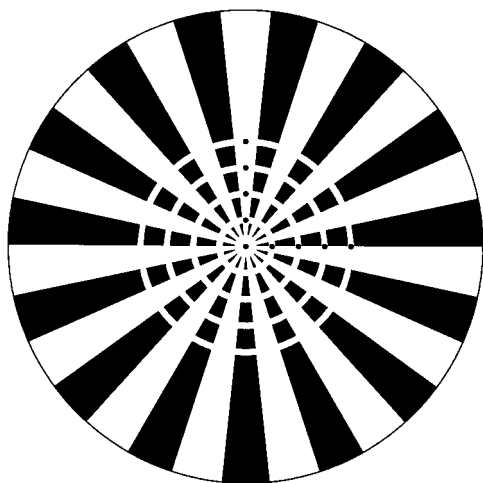


FIG. 1. Roll optokinetic stimulus used to induce a torsional offset. The surface was equally divided into 30 radial segments with an alternating black and white pattern. The radius of the disk was 48 cm, subtending  $40^\circ$  from its center. Four circular strips were pasted on the surface concentrically at eccentricities of 5, 10, 15, and  $20^\circ$  to prevent intensity modulation of laser targets during the disk rotation. Lights from 2 lasers were used as saccade targets (presented at loci indicated with 9 small circles) to elicit horizontal and vertical saccades.

### Optokinetic stimulus

A rotating circular flat disk (Fig. 1) was used for optokinetic stimulation and so induced torsional errors. The disk was positioned in front of the subjects, 0.52 m from their eyes with the center of the disk at eye level. At this distance the radius of the disk was  $40^\circ$ . The surface of the disk was equally divided into 30 radial segments with an alternating black and white pattern. White circular strips were concentrically pasted on the surface at eccentricities of 5, 10, 15, and  $20^\circ$  to prevent intensity modulation of laser targets during the disk rotation. Two lasers were used to elicit horizontal and vertical saccades. The light from one laser was projected to the center of the disk and from the other projected to one of eight loci spaced  $5^\circ$  apart rightward or upward from the center as shown in Fig. 1. A motor rotated the disk clockwise or counterclockwise at a constant velocity of either 10 or  $30^\circ/\text{s}$ .

### Eye movement recording

Movements of both eyes about all three rotation axes were simultaneously recorded using dual search coils (Skalar, Netherlands). The description of the coil system and its calibration can be found in Straumann et al. (1995). In brief, three pairs of field coils were wound in a cubic frame (Remmel 1984), with the length of each side 1.02 m. Voltage offsets were nullified with the scleral annuli placed in a metallic tube. For a calibration, the maximal voltages induced in each of the two detection coils by the three magnetic fields were determined by aligning the sensitivity vector of the detection coils with the three orthogonal field coil axes, using a gimbal system located at the center of the field coil frame. Signals from the annuli were phase-detected (field frequencies of 55.5, 83.3, and 42.6 kHz), and the analog signals from the corresponding 12 channels were sampled at a rate of 500 Hz with a resolution of  $<0.1^\circ$  (peak-to-peak noise level). These signals were then normalized to the maximal voltage vectors, and the sensitivity vectors of the direction and torsion coils were orthogonalized. Rotation vectors were calculated to describe the three-dimensional orientation of the scleral annuli (Haustein 1989). We shall describe the three components of rotation vectors in angular degrees whereby  $x$ ,  $y$ , and  $z$  describe the torsional, vertical, and horizontal directions, respectively. According to the right-hand rule, leftward, downward, and extorsion of the right eye and intorsion of the left eye are positive.

### Experimental procedures

Subjects were seated inside the coil frame so that the center of the interpupillary line was aligned with the center of the frame. After the conjunctiva was anesthetized with a few drops of 0.5% proparacaine hydrochloride, the dual search coils were mounted on the eyes. The head was held still with a bite bar and dental impression material. The optokinetic disk (Fig. 1) was placed in front of the subject at the opening of the coil frame. Featureless black cardboard and black curtains covered the top and side openings of the coil frame. Each subject participated in two recording sessions: one for a horizontal and the other for a vertical series of saccades. In each session, subjects participated in the three paradigms explained below with both eyes viewing.

**PARADIGM 1.** This was the main experimental paradigm, and its purpose was to compare torsional components of saccades made with and without the torsional offset induced with the optokinetic disk (Fig. 2). Subjects made saccades between two laser targets: one at the center of the disk and the other at one of four eccentricities, 5, 10, 15, and  $20^\circ$ , to the right (horizontal series), or up (vertical series). Brief tones (arrows in Fig. 2) signaled when subjects were to make a saccade to the eccentric target and a pair of brief tones signaled when to make saccades back to the center target. A trial started with subjects fixing on the laser target at the center of the disk. Fifty percent of the centrifugal saccades toward eccentric laser targets were made in an otherwise completely dark room without any torsional offset. These saccades will be referred to as *D-saccades*. Before the remaining 50% of the centrifugal saccades, the rotating optokinetic disk was made visible for a few seconds so that the torsional position of the eye was

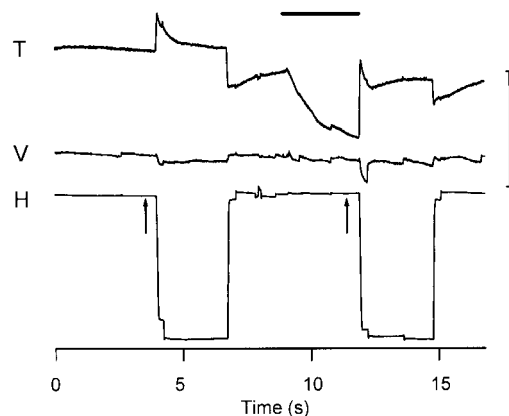


FIG. 2. Trial of *paradigm 1*. Horizontal ( $H$ ), vertical ( $V$ ), torsional ( $T$ ) components of the rotation vectors describing the position of the right eye are plotted. The calibration bar is  $5^\circ$  for  $T$  and  $V$  traces, and  $15^\circ$  for  $H$  trace. Rightward movements are indicated by downward movement of the trace. The trial started with the subject fixing on the center laser target. Beeps, indicated by arrows, signaled when the subject was to make a saccade, in this case to a laser target at  $20^\circ$  to the right. The 1st rightward saccade (immediately after the left arrow, *D-saccade*) was made in the dark, and the 2nd one (after the right arrow, *L-saccade*) was also made in the dark, but after a torsional offset was induced by the optokinetic nystagmus (OKN) disk. Top horizontal bar indicates the duration of the overhead light being ON, and thus the disk visible, rotating at  $30^\circ/\text{s}$  counterclockwise in this example. The intorsion (downward deflection) of the right eye in the  $T$  trace can be seen during the light ON period, which was then corrected during a subsequent saccade. The light went off when the horizontal centrifugal saccade rotated the eye beyond the  $2^\circ$  window about the center. The duration of the light being ON, thus consisted of a fixed 2.5-s period before the beep plus the interval from the beep to when the eye left the window. The eye remained at the eccentric target (for 2.5 s plus a random period between 0 and 1 s); 2 consecutive beeps (not indicated) with a brief separation (10 ms) signaled the subject to make a saccade back to the central laser target. The time between the return to the center target and the next trial was 2 s plus a random period between 0 and 1 s. The above trial was repeated 4 times within a block.

driven out of the resting position, i.e., away from Listing's plane. The single tone then sounded to signal the time to make the centrifugal saccades. The overhead light went off when the eye position broke a  $2^\circ$  electronic window around the center target, i.e., just after the saccade began. These saccades will be referred to as *L-saccades*. For each saccade eccentricity, four conditions were used: two disk speeds (10 or  $30^\circ/\text{s}$ ) and two directions of disk rotation [clockwise (CW) or counterclockwise (CCW)], relative to the experimental subject. The location of the eccentric laser target was changed between blocks by a computer-driven mirror galvanometer. Within a session (horizontal or vertical), there were 20 blocks (5 amplitudes  $\times$  2 directions  $\times$  2 speeds), each consisting of four continuous repetitions of the trial shown in Fig. 2. Thus from a single successful block four D-saccades and four L-saccades were collected.

The 12 channels of analog eye position data, outputs from a tachometer from the motor rotating the disk and from a photodiode pointing at the surface of the edge of the disk and registering its speed of rotation, were stored. The ON/OFF state of the overhead light that was used to illuminate the rotating disk, and the sound of the tone signal, were digitized at a rate of 500 Hz and also stored. The direction of disk rotation was reversed between blocks and the order in which the eccentric laser targets were illuminated was 10, 5, 20, and  $15^\circ$ . The mean decay time constant of the output of the photodiode when the overhead light went off in 10 representative trials, was 18.16 ms ( $\pm 0.65$ ), indicating that the overhead light did not produce any transient afterglow when it went off.

**PARADIGM II.** In this paradigm, subjects fixed on the center target while the disk was rotating, and no saccades were made. While subjects were fixing on the central target, the overhead light went on and off. The purpose of this paradigm was to examine the time course of passive recovery in torsional eye positions, and to obtain data on the dynamic properties of pure torsional quick phases.

**PARADIGM III.** This paradigm was the same as *paradigm I*, except that the overhead light stayed on during centrifugal saccades. The purpose of this paradigm was to evaluate the effect of extinguishing the light during saccades on the corrective torsional movements. Four blocks of data were collected using this paradigm for each session: two speeds  $\times$  two directions of disk rotation  $\times$  one saccade amplitude of  $10^\circ$ .

Before and after each experimental session, data for fitting Listing's plane were collected while subjects fixed on six small dots marked on the resting optokinetic disk, equally spaced apart at  $12.5^\circ$  of eccentricity.

### Data analysis

Rotation vectors describing three-dimensional eye position were calculated every 4 ms with  $[0,0,0]$  taken as the first sample of the session during fixation of the central target. To determine the amount of torsion specifically associated with saccades, called the "dynamic" torsion, we corrected for changes in static torsion that simply depended on static horizontal and vertical positions of the eye by subtracting the "false" torsion that depends on the choice of the reference position, so-called reference-position-dependent torsion (Suzuki et al. 1994). This procedure, described elsewhere (Straumann et al. 1995), is equivalent to analyzing the trajectories after rotating the eye position data such that Listing's plane is perpendicular to the head-fixed coordinate system. For each block of *paradigm I*, the torsional components of rotation vectors before, and 2 s after the onset of the saccade made to the eccentric target, were obtained to be used for the correction for any change in static torsion. Any dynamic torsion then was defined as the deviation from this estimate of static torsional position.

A displacement vector,  $d$ , was calculated to describe the magnitude of the three-dimensional change of eye position from  $r_1$  to  $r_2$  positions as follows (Van Opstal 1993)

$$d = (r_2 - r_1 + r_1 \times r_2) / (1 + r_1 r_2)$$

where  $r_1$  and  $r_2$  are rotation vectors, and  $\times$  the vector cross product. Three-dimensional eye angular velocity vectors,  $\omega$ , that take into account both the current eye position,  $r$ , and its time derivative,  $r'$ , were calculated as follows (Hepp 1990)

$$\omega = 2 * (r' + r \times r') / (1 + r^2)$$

The onset and offset times of horizontal or vertical saccades were determined with a velocity criterion. The peak torsional velocity was defined as the peak of the torsional component of angular velocity vectors during horizontal or vertical saccadic eye movements.

## RESULTS

### Torsional correction

Figure 3 shows representative data obtained from one block of four trials. Saccades to a laser target at  $20^\circ$  to the right, without (*left panels*) and with (*right panels*) torsional offsets are illustrated. The torsional offset was introduced by the optokinetic disk rotating counterclockwise (CCW) at  $30^\circ/\text{s}$ , thus intorting the right eye (pulling T position negatively). The torsional (T, *top panels*) and horizontal (H, *bottom panels*) components are each superimposed. The saccades made in the dark (without the torsional offset, D-saccades) show a torsional component (*top left panel*), the so-called blip, which transiently moves the eye out of Listing's plane during saccades (Straumann et al. 1995). For L-saccades, shown in the *right panels*, the "torsional error" is defined as an offset from the zero torsion value indicated by a horizontal line. This zero torsion value was virtually identical to the torsional component of the

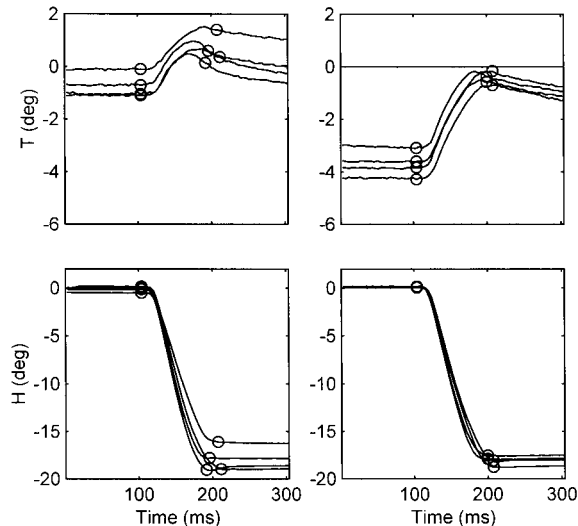


FIG. 3. Representative saccades from a block of 4 trials (right eye) including the one trial shown in Fig. 2. Saccades made to the same target ( $20^\circ$  to the right) without (*left panels*) and with (*right panels*) a torsional offset, were isolated and their torsional (T, *top panels*) and horizontal (H, *bottom panels*) components were each superimposed, aligned at saccade onset. The onset and offset of saccades, as determined from the velocity of the horizontal component, are indicated with circles. The OKN disk was rotating  $30^\circ/\text{s}$  counterclockwise, thus intorting the right eye before the saccade was made (*top right panel*). Extorsion of the right eye is positive in T, and the rightward movement is negative in H. Note that the zero torsion is torsional eye position when 1<sup>st</sup> sampled while the subjects fixed on the central target, which in this case was calculated to be  $0.06^\circ$  positive relative to the primary position, that is, the line of sight perpendicular to Listing's plane. Thus the zero torsion value in the figure closely corresponds to an eye position in Listing's plane.

primary eye position based on the orientation of Listing's plane (also see the legend to Fig. 3). One can see that the torsional error was minimized while the saccade was being made. This torsional movement reflects the sum of both the torsional blip associated with the saccade itself and the reduction of the torsional offset that had been induced by the optokinetic disk. In this condition (CCW rotation) these two components work in the same direction to rotate the eye back toward zero torsion.

Figure 4 illustrates the torsional components associated with rightward saccades of varying amplitudes. The four panels in the *left column* show the torsional components of horizontal *D-saccades* toward targets at various rightward eccentricities (5, 10, 15, and 20°). The torsional blip increased as horizontal saccade amplitude increased, as previously described by Straumann et al. (1995). Here, the blips extort the right eye during the saccades. The *right panels* show the torsional components of L-saccades that were made after torsional offsets were induced with the optokinetic disk rotating at 30°/s CCW. During horizontal saccades (short horizontal bars at *bottom of each panel*), the torsional offset (approximately  $-3^\circ$ ) was reduced by a corrective torsional movement that was in the same direction (positive) as the torsional blip. For small horizontal saccades, e.g., 5°, the torsional offset (i.e., error from

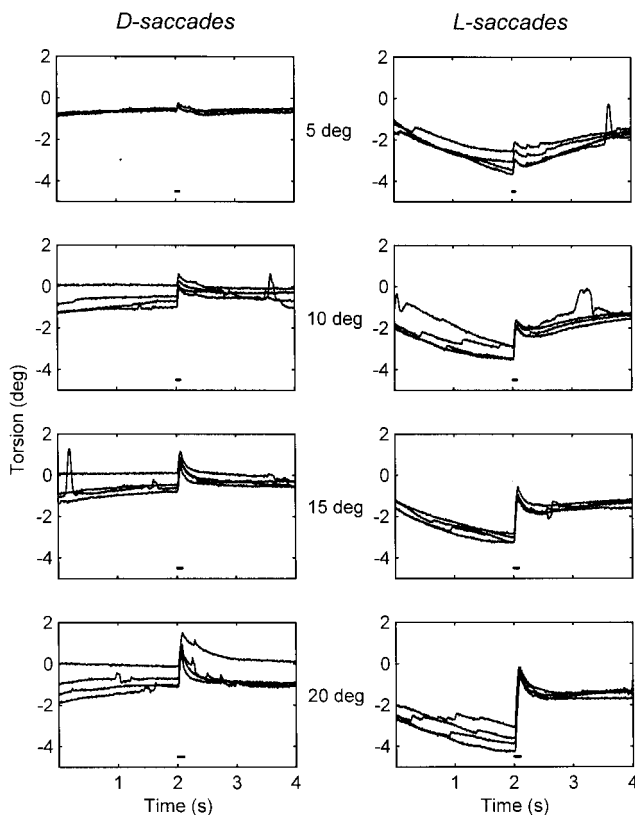


FIG. 4. Torsional components of saccades made to targets at 4 different eccentricities (5, 10, 15, and 20°) to the right, without (*D-saccades*) and with (*L-saccades*) torsional offset induced with the disk rotating at 30°/s in the counterclockwise direction. Data for the right eye from four blocks from one subject (*CL*) are compiled. Saccades toward a 20° target (*bottom 2 panels*) are also shown in Fig. 3. In all panels, traces are superimposed at saccade onset at 2 s. The abrupt positive-going segments starting at 2 s roughly corresponds to the duration of horizontal saccades, which is indicated by short horizontal bars starting at 2 s and spanning the mean duration of horizontal saccades. The zero torsion in all panels is within 0.1° from the torsional component of the primary eye position.

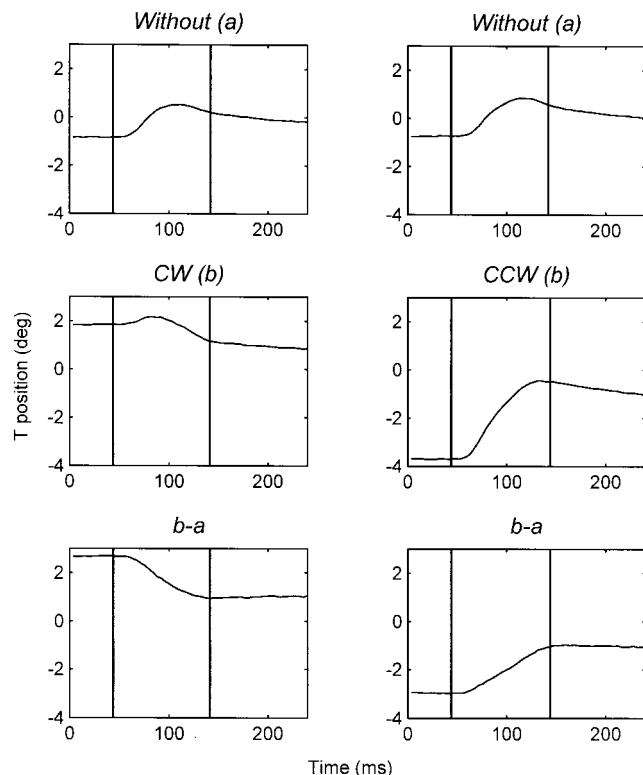


FIG. 5. Time course of the blip-subtracted torsional movement in a representative subject (*CL*). The OKN disk was rotating at 30°/s clockwise (*CW*, *left column*) and counterclockwise (*CCW*, *right column*). Saccades were made toward a laser target at 20° to the right in the dark without (*top panels*) and with (*middle panels*) a torsional offset. The trace in each panel is an average of 4 saccades obtained in the same block. For averaging purposes, all torsion traces were aligned at the onset of the horizontal saccade (left vertical bars). The right vertical bar in each panel is the offset of the horizontal saccade determined from the mean duration of horizontal saccades. The mean durations for the “Without” and “CW” in the *left panel* are 90 and 98 ms, but the differences were not consistently observed, and in the *right panel* they were 95 ms in both conditions. Note that the asymmetry in torsion (*middle panels*) largely disappears after subtracting the blip (*bottom panels*,  $b - a$ ). To calculate the time constant of the blip-subtracted torsion (see text), a segment of  $b - a$  from the peak torsional velocity (spanning  $\sim 100$  ms) was fitted with an exponential function with a single time constant using an optimization routine provided by Matlab (the MathWorks).

zero torsion) was not fully corrected, and the residual torsional error was slowly corrected after the saccade while fixing on the eccentric target.

To reveal the corrective torsional movement in the L-saccades, the mean trace of the torsional blip from the *D-saccades* was obtained and subtracted from that of the torsional component of L-saccades (Fig. 5). Due to the torsional blip of *D-saccades*, which first extorted the eye (Fig. 5, *top panels*), the torsional component of L-saccades appeared asymmetric between the clockwise (*CW*) and *CCW* conditions (Fig. 5, *middle panels*). After the effect of the torsional blip was removed, however, the asymmetry in the magnitude of the torsion was greatly reduced (Fig. 5, *bottom panels*). The blip-subtracted torsion ( $b - a$ ), thus reflects corrective torsional movements; intorting in *CW* and extorting in *CCW* disk rotation conditions.

The blip-subtracted torsional movements during saccades (*bottom panels*,  $b - a$ , of Fig. 5) were fast; their time constants were 19 ms in *CW* and 25 ms in the *CCW* conditions. Thus

recovery from extorsion was slightly faster in this condition, but in other conditions, when different target amplitudes and disk speeds were used, recovery from intorsion could be slightly faster. For example, in the condition when saccades were made toward  $10^\circ$  to the right with the OKN disk rotating at  $10^\circ/\text{s}$  (in the same subject, *CL*), the time constants of the blip-subtracted torsional corrections were 28 ms in the CW and 17 ms in the CCW conditions. There was inter- and within-subject variability in these time constants; *subject MH* showed the fastest torsional movement and in the same condition as Fig. 5, the time constants of  $b - a$  were 7.5 ms in CW and 9 ms in CCW conditions. Time constants for *subject DZ* were 12 and 27, and for *subject NH* were 20 and 24 ms for CW and CCW conditions, respectively. The overall mean time constant was  $18 \pm 7.4$  (SD) ms. The time constants of the blip-subtracted torsional correction were comparable for vertical saccades (mean,  $24 \pm 14$  ms).

To determine whether the blip-subtracted torsional correction has the dynamic characteristics as saccades, the main sequence of the blip-subtracted torsion was examined. On Fig. 6, the main sequence relationships (peak velocity as a function of amplitude) of blip-subtracted torsional movements during L-saccades (in *paradigm I*) and torsional movements during torsional quick phases (in *paradigm II*) are compared for all four subjects. In all cases, the OKN disk was rotating at  $30^\circ/\text{s}$ . The peak torsional velocity of torsional quick phase (circles) was comparable to the blip-subtracted torsion during L-saccades toward horizontal targets (asterisks), matched for torsional amplitude. In each panel, a best-fit line was drawn through the asterisk points. The mean of the slopes was 24.3

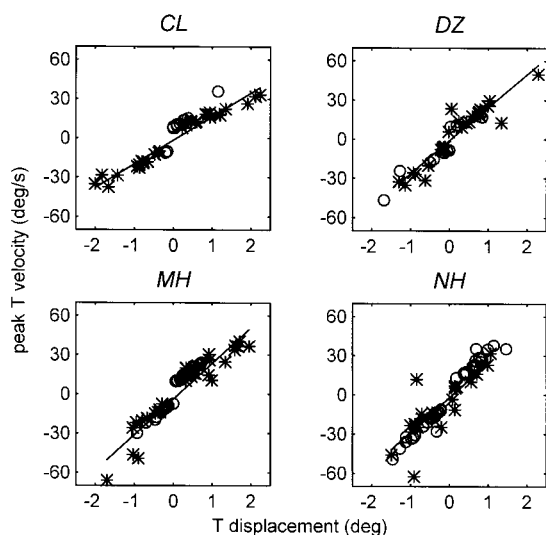


FIG. 6. Comparison of main-sequence plots between torsional movements during saccades and torsional quick phases during optokinetic nystagmus. Data from all 4 subjects are plotted. Each asterisk represents peak torsional velocity after subtracting the blip torsion, combining all saccades made toward 4 horizontal targets using the disk rotating at  $30^\circ/\text{s}$ . Positive displacement and velocity are from the CCW, and negative displacement and velocity from the CW conditions. The line in each panel is the least-square fit through the asterisks. Each circle represents a torsional quick phase obtained from *paradigm II* in which fixation was maintained on the central laser while the disk was rotating at  $30^\circ/\text{s}$  CCW (1st quadrant) and CW (3rd quadrant). Note that the peak torsional velocities of quick phase movements (circles) were comparable to that of the torsional component of saccades toward horizontal targets, for matching displacements. The slopes of the lines are 18.11, 25.32, 27.24, and 26.54 (deg/s)/deg, for *CL*, *DZ*, *MH*, and *NH*, respectively.

(deg/s)/deg. A similar pattern of relationship between the peak torsional velocity and torsional displacement was found for quick phases in response to the  $10^\circ/\text{s}$  optokinetic stimulus alone; there were no differences between the slope and intercept of the best-fit line through this quick phase data and the torsional data from *paradigm I* (asterisks). The peak torsional velocities obtained in this study were similar to those reported for torsional saccades by Collewijn et al. (1985).

#### Effects of the speed of disk rotation

For L-saccades, we pooled all the data from all subjects and stimulus conditions for the disk rotating at  $10^\circ/\text{s}$  (229 L-saccades) and  $30^\circ/\text{s}$  (232 L-saccades), and calculated the mean torsional component at saccade onset. This value was subtracted from the mean torsional eye position at the onset of D-saccades to obtain a measure of the stimulus-induced torsional deviation prior to L-saccades. Similarly, the mean of the torsional component during the D-saccades was subtracted from the torsional component of the displacement vector defined by rotation vectors at the onset and offset times of horizontal or vertical L-saccade to obtain the stimulus-induced torsional movement. The initial torsional deviation and the magnitude of the torsional component of blip-subtracted L-saccades are presented in Table 1. The effect of the OKN disk on initial torsional deviation was variable among subjects ( $F_{3,453} = 157.25$ ,  $P < 0.001$  for right eye and  $F_{3,453} = 124.57$ ,  $P < 0.001$  for left eye). The mean initial torsional deviation of blip-subtracted L-saccades made for the right eye in the  $10^\circ/\text{s}$  disk rotation condition was  $1.11 \pm 0.68^\circ$  and in the  $30^\circ/\text{s}$  condition,  $1.46 \pm 1.05^\circ$ . For the left eye, the value for  $10^\circ/\text{s}$  disk rotation was  $0.96 \pm 0.63^\circ$  and for the  $30^\circ/\text{s}$ ,  $1.21 \pm 0.96^\circ$ . This difference in initial torsional deviation between the two disk speeds was statistically significant ( $F_{1,453} = 38.26$ ,  $P < 0.001$  for the right eye,  $F_{1,453} = 20.37$ ,  $P < 0.001$  for the left eye). In contrast to the other three subjects, for *subject NH* there was little effect of disk speed.

#### Initial torsional offset and magnitude of torsional correction

To determine whether the magnitude of torsional correction is related to the initial torsional offset, the blip-subtracted torsional displacement of L-saccades was plotted as a function of the initial torsional position (Fig. 7). For both eyes making both horizontal and vertical saccades, if the initial torsional deviation was larger, then the torsional movement during the saccade was larger. Note that both the initial torsional position and torsional magnitude were normalized with respect to D-saccades, and thus the initial torsional position reflects the stimulus-induced torsional offset, and the torsional magnitude reflects the amount of correction of torsional error that was induced by the stimulus. The correction was not perfect (Table 1, Fig. 7); the slope relating the torsional magnitude to initial torsional position was approximately  $-0.5$ , indicating that  $\sim 50\%$  of the initial torsional offset was corrected during the primary saccade in our experimental paradigm. The torsional correction was 8% larger for vertical saccades than for horizontal saccades, as estimated by the difference in the slope given in the legend to Fig. 7.

The ratio of torsional magnitude to initial torsional offset (T correction ratio) was related to saccade duration and amplitude

TABLE 1. Mean initial torsional deviation and mean torsional displacement

Subject	<i>n</i> (10/30)	Right Eye				Left Eye			
		Initial T position		T magnitude		Initial T position		T magnitude	
		10	30	10	30	10	30	10	30
<i>CL</i>	61/60	1.78 ± 0.55	2.37 ± 0.71	0.75 ± 0.46	1.02 ± 0.56	1.62 ± 0.42	2.19 ± 0.57	0.75 ± 0.50	0.94 ± 0.49
<i>DZ</i>	57/58	1.18 ± 0.58	2.00 ± 1.02	0.56 ± 0.42	0.97 ± 0.59	0.79 ± 0.70	1.30 ± 1.10	0.52 ± 0.45	0.78 ± 0.56
<i>MH</i>	61/59	0.92 ± 0.43	1.01 ± 0.57	0.58 ± 0.38	0.78 ± 0.54	0.87 ± 0.33	0.93 ± 0.51	0.49 ± 0.34	0.72 ± 0.49
<i>NH</i>	50/55	0.46 ± 0.38	0.38 ± 0.34	0.56 ± 0.46	0.55 ± 0.33	0.48 ± 0.38	0.35 ± 0.31	0.48 ± 0.40	0.57 ± 0.37
Total	229/232	1.11 ± 0.68	1.46 ± 1.05	0.62 ± 0.43	0.83 ± 0.54	0.96 ± 0.63	1.21 ± 0.96	0.56 ± 0.44	0.76 ± 0.50

Values are means ± SD in degrees; *n* (10/30) indicates number of L-saccades in conditions of 10°/s and 30°/s of disk speed. Saccades from clockwise (CW) and counterclockwise (CCW) conditions in both horizontal and vertical saccade series were combined after absolute values of initial torsional (T) position in CCW and T magnitude in CW conditions were taken because they were mostly negative values. Numbers under Initial T Position are mean initial torsional deviations in degrees of L-saccades with respect to D-saccades at the beginning of horizontal and vertical saccades. Numbers under T magnitude are the difference in torsional displacement in degrees between L-saccades and D-saccades during horizontal and vertical saccades. There were no statistically significant differences in initial T position ( $F_{1,459} = 1.39$ ,  $P = 0.24$ ), or in T magnitude ( $F_{1,459} = 1.18$ ,  $P = 0.28$ ) between the horizontal and vertical series, and so the data are accordingly combined.

(Fig. 8). The slope relating this ratio to saccade duration was higher for horizontal than for vertical saccades (Fig. 8A), but this could be due to the fact that saccade duration was considerably lower for horizontal than for vertical saccades as can be seen in Fig. 8A. When the same ratio was plotted as a function of saccade amplitude, the slopes became closer (Fig. 8B). The linear regression equation relating the ratio of torsional correction to saccade amplitude for horizontal saccades, combining

all subjects was  $y = 0.0387x + 0.1537$ , and that for vertical saccades was  $y = 0.0283x + 0.3658$ . The slopes of the linear regression equations for combined horizontal and vertical saccades for each subject were 0.0321 (*CL*), 0.0341 (*DZ*), 0.0375 (*MH*), and 0.0379 (*NH*), and that combined for horizontal and vertical saccades for all subjects was  $y = 0.0318x + 0.2829$ . This suggests that approximately 3.18% of the torsional deviation is corrected per degree of horizontal or vertical saccade. Thus in addition to the initial torsional deviation, saccade amplitude appears to be a major predictor of the amount of intrasaccadic torsional correction. Furthermore, the fact that the ratio is higher for vertical than for horizontal saccades (Figs. 7 and 8B) suggests that saccade duration is also related to the amount of torsional correction, and that a saccade provides a temporal window within which the initial torsional offset is corrected.

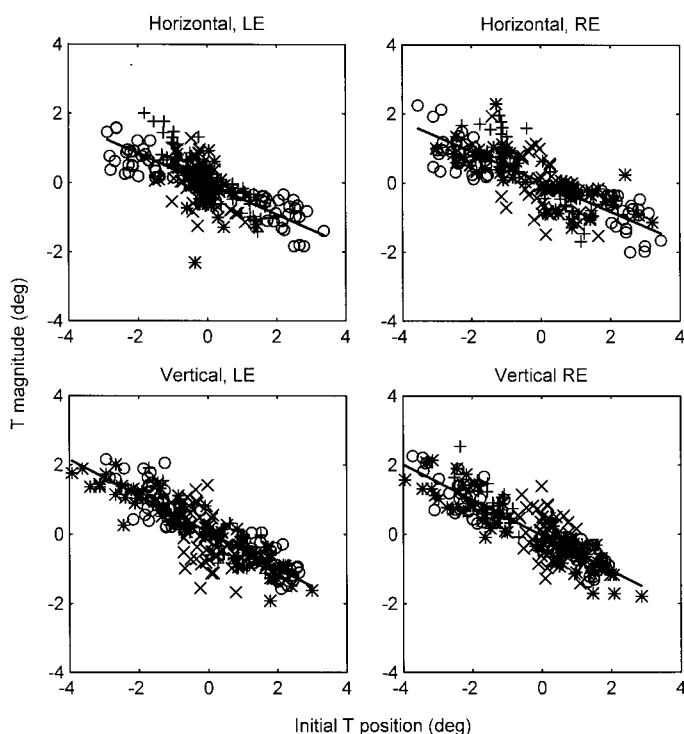


FIG. 7. Torsional displacement of L-saccades as a function of the initial torsional position for left (LE) and right (RE) eyes from horizontal (top) and vertical (bottom) series. In each panel, on the ordinate is the magnitude of blip-subtracted torsional displacement and on the abscissa is the initial torsional deviation of L-saccades from the initial torsional position of D-saccades. Each symbol represents each L-saccade for *subject CL* (○), *DZ* (\*), *MH* (+), *NH* (×). The linear regression lines are  $y = -0.44x - 0.03$  (Horizontal, LE,  $R^2 = 0.58$ ),  $y = -0.43x + 0.04$  (Horizontal, RE,  $R^2 = 0.63$ ),  $y = -0.52x + 0.06$  (Vertical, LE,  $R^2 = 0.73$ ), and  $y = -0.51x - 0.03$  (Vertical, RE,  $R^2 = 0.77$ ).

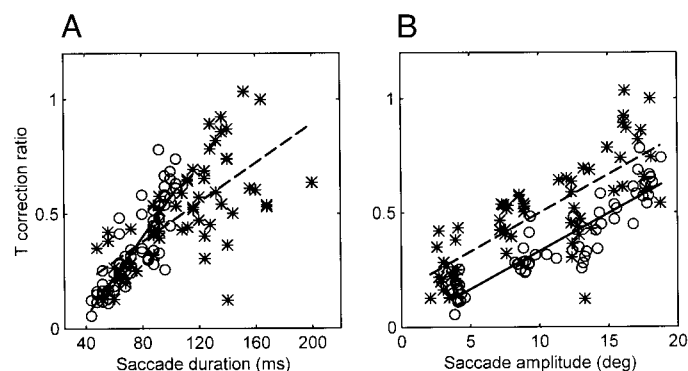


FIG. 8. Ratios of torsional correction as functions of saccade duration (A) and saccade amplitude (B) for *subject CL*. In both panels, each symbol represents the ratio of blip-subtracted torsional displacement to the initial torsional offset of one horizontal (circle) or vertical (asterisk) L-saccade. Solid and dashed lines are linear regression lines for horizontal and vertical saccades, respectively. Equations of these lines in A are  $y = 0.0087x - 0.2977$  (—) and  $y = 0.0043x + 0.0333$  (---), and in B,  $y = 0.0331x - 0.0005$  (—) and  $y = 0.0336x + 0.1608$  (---). The linear regression equations for combined horizontal and vertical saccades for each subject after eliminating outliers with the correction ratio exceeding 2, were  $y = 0.0321x + 0.0938$  (*CL*),  $y = 0.0341x + 0.1889$  (*DZ*),  $y = 0.0375x + 0.3081$  (*MH*), and  $y = 0.0379x + 0.5443$  (*NH*), where  $x$  is saccade amplitude and  $y$  is the ratio of the torsional correction.

### Torsional velocity

Figure 9 shows the trajectory of the torsional component of the angular velocity vectors for rightward saccades of *subject CL*. Saccades were made to a target  $15^\circ$  to the right. In the *top left panel*, torsional blip velocity is shown for horizontal D-saccades. Due to the asymmetry in torsional blip velocity (CW early, CCW late), the torsional velocity traces of L-saccades are different between the CW and CCW torsional offset conditions (*middle and bottom, left panels*). In the *right panels*, the torsional velocities of L-saccades in the CW and CCW conditions are shown after the effect of the torsional blip was subtracted. With this subtraction, the absolute values of peak torsional velocity can be compared between the L-saccades in the CW and the CCW conditions.

The peak torsional velocity, after subtracting the blip torsion, increased with the speed of rotation of the disk; the peak torsional velocity of blip-subtracted L-saccades combined for horizontal and vertical series for all subjects was  $13.5^\circ/\text{s}$  for the  $10^\circ/\text{s}$  OKN disk speed, and  $18.1^\circ/\text{s}$  for the  $30^\circ/\text{s}$  disk speed. This difference in peak torsional velocity was probably related to the difference in the initial torsional deviation described above. Thus peak torsional velocity, corrected for the blip, reflects the parameters of stimulation, in much the same way as the magnitude of the blip-subtracted torsion increased with the

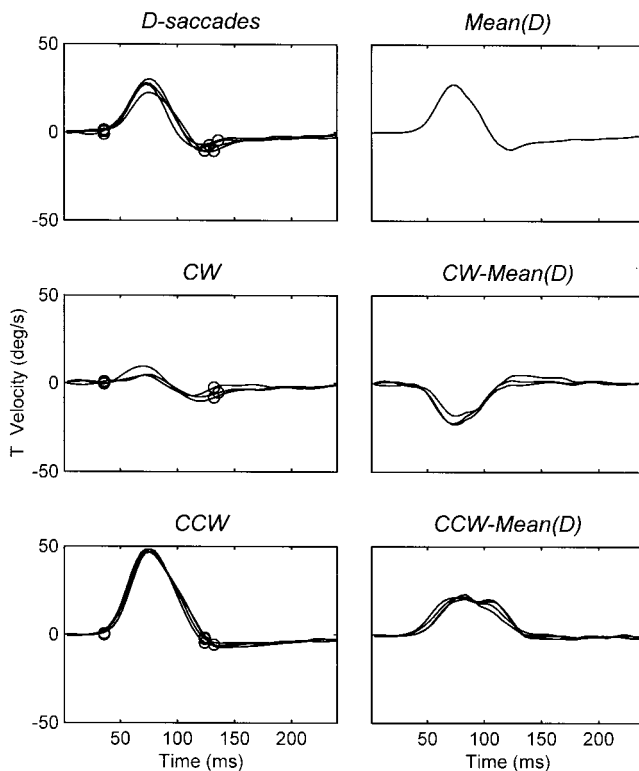


FIG. 9. Torsional velocity. *Left panels*: torsional components of angular velocity vectors of saccades made by the right eye of one subject (*CL*), without (*D*) and with (*CW*, *CCW*) torsional offset, are superimposed and aligned at saccade onset (1st circles). The OKN disk was rotating at  $30^\circ/\text{s}$  in a *CW* or *CCW* direction. In all cases, saccades were made to a target at  $15^\circ$  to the right. Due to the asymmetry of the torsional blip associated with the saccade itself (*D*), the torsional velocity traces are different between the *CW* and *CCW* conditions. *Right panels*: the effect of the torsional blip is removed, by subtracting the mean torsion of D-saccades [*Mean(D)*] from the L-saccade traces in *CW* and *CCW* conditions. A more symmetrical torsional component between L-saccades in the 2 conditions is now apparent.

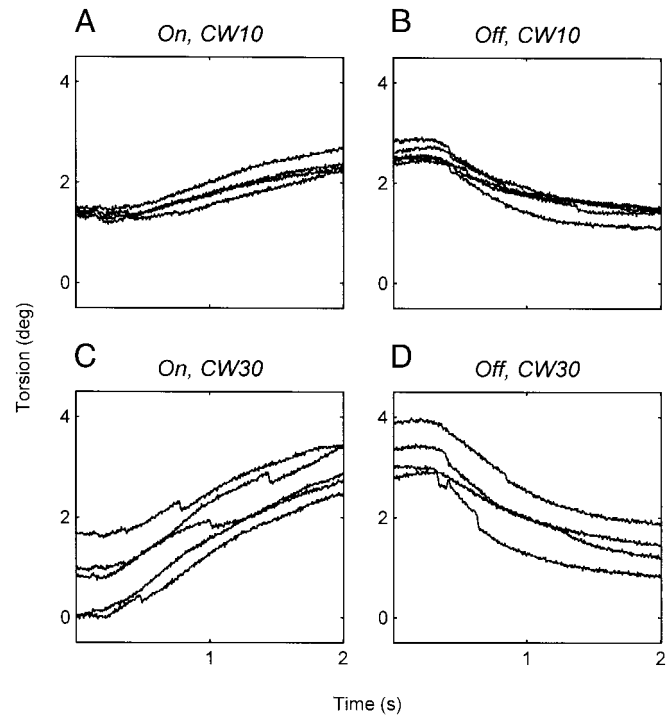


FIG. 10. Recovery of torsional offset without a saccade in a representative *subject CL*. The OKN disk was rotating at  $10^\circ/\text{s}$  in clockwise in *A* and *B*, and  $30^\circ/\text{s}$  in clockwise in *C* and *D*. While the eyes fixated on the center of the disk, an overhead light went on and off. The torsional component of the rotation vectors are superimposed, aligned at onset (*A* and *C*) and offset (*B* and *D*) of the light, at time 0. The latency of torsional following is larger than 200 ms. The time constants of the change in torsional position are larger than 380 ms in all cases.

speed of the OKN disk. Accordingly, we can divide the saccade-related torsion into two components: blip torsion and stimulus-induced torsion. The peak torsional velocity of blip-subtracted L-saccades increased with horizontal or vertical saccade amplitude, and this is related to the fact that the intrasaccadic torsional change increased with saccade amplitude (Fig. 8).

### Control experiments

Since a major question about our results is whether or not the movements that correct for torsional offset during saccades simply reflect passive recovery due to muscle mechanics, we did two control experiments. First, we examined the return of torsion to its baseline value in the absence of saccades using *paradigm II*, in which the optokinetic disk was alternately visible and invisible while the eyes maintained fixation on the central target (Fig. 10). The periods immediately after the light OFF, and free of saccades or quick phases, were isolated and the time constants of return of torsional position to baseline were calculated by fitting an exponential function (see legend to Fig. 5). Twenty-three traces from three subjects [data from one subject (*NH*) showed too many quick phases to be included] were analyzed for this purpose. The mean time constant for the right eye across all subjects was  $740 \pm 325$  ms, and that of the left eye was  $766 \pm 566$  ms. This difference was not statistically significant. There were also no statistically significant differences in the time constants between the *CW* and *CCW* conditions ( $P > 0.64$  for the right eye and  $P > 0.37$  for the left eye).

In *paradigm III*, the effects of illumination of the background on torsional movements were examined. The overhead light stayed on during saccades, and the torsional component of these saccades was compared with that obtained in *paradigm I*, in which case the light went out when the saccade began. Regardless of the visibility of the optokinetic disk, the associated torsion during and immediately after the saccade followed the same stereotypical trajectory to approximately 240 ms after the onset of the saccade (Fig. 11) for both disk speeds.

#### Conjugacy of torsional movements

Torsional movements of D-saccades were asymmetric; blip torsion was bigger in the right eye during rightward saccades and bigger in the left eye for leftward saccades (not shown); thus there was a transient blip-associated cyclovergence as reported by Straumann et al. (1995). During L-saccades, torsional movements actively corrected the OKN-induced torsional error as described above, and these movements were conjugate. In this condition, the magnitude of the torsional

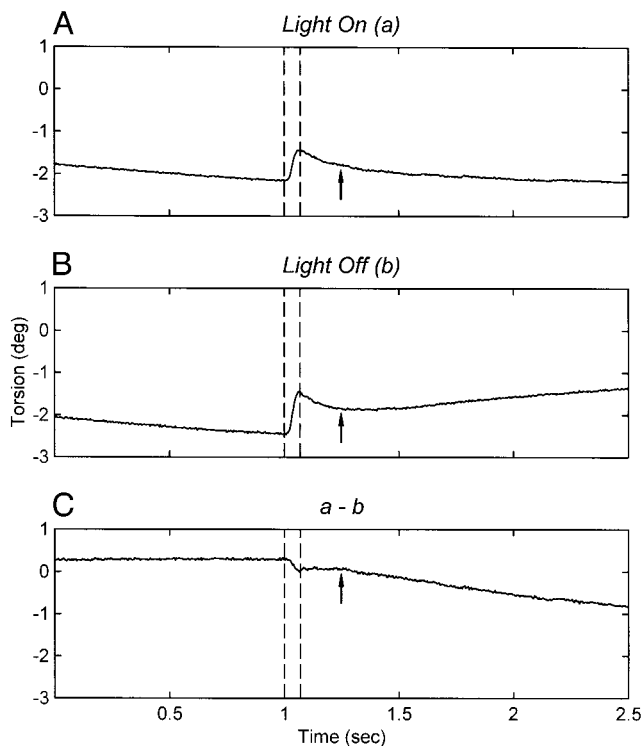


FIG. 11. Effects of turning the light off on torsional movements. The subject made saccades to a target at  $10^\circ$  to the right, while the OKN disk, rotating at  $10^\circ/\text{s}$  in CCW, was visible continuously (A) or was extinguished immediately after the onset of saccade (B). In A and B, the mean torsion traces of 5 saccades (aligned at saccade onset) are plotted. The 1st vertical dashed line indicates saccade onset, as determined from the horizontal movement. The mean saccade duration was obtained, and thus the saccade offset is indicated by the 2nd vertical dashed line. The bottom panel ( $a - b$ ) plots the difference between the two. The torsional movements are the same up to the point indicated by an arrow (240 ms after the onset of saccade). This point is also indicated in A and B. The small intrasaccadic difference probably reflects the difference in initial torsional position between A and B. The monotonic torsional movement after the saccade in A reflects torsional visual following. At this time, the eye was fixing on the eccentric target ( $10^\circ$  to the right in this case). The time indicated by the arrow in C was determined at the X-axis intercept of the linear regression line. To subtract static torsion (dependent on horizontal position), the T/H slope obtained from the session of CW  $10^\circ/\text{s}$  with the target amplitude of  $10^\circ$ , was used.

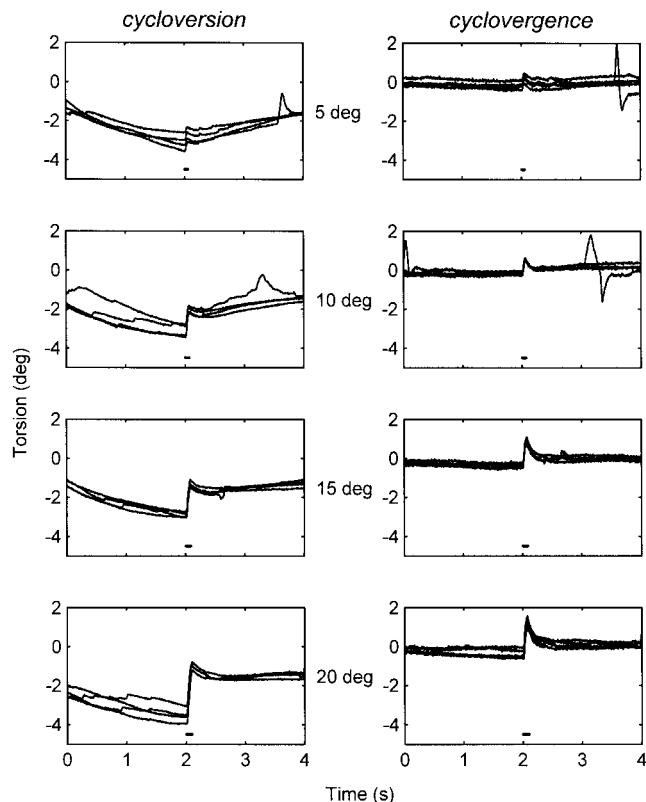


FIG. 12. Cycloverversion (left) and cyclovergence (right) of L-saccades made toward horizontal targets of  $5^\circ$ ,  $10^\circ$ ,  $15^\circ$ , and  $20^\circ$  to the right for *subject CL* with the disk speed of  $30^\circ/\text{s}$  in CCW. Cycloverversion is defined as right eye torsion plus left eye torsion, divided by 2 and cyclovergence is defined as right eye torsion minus left eye torsion. The abrupt version and vergence movements starting at 2 s correspond to the duration of horizontal saccades (short horizontal bars). Note that the transient cyclovergence during the saccade is due to asymmetric blip torsion; considerably larger in the right eye than in the left eye.

component was different between the right and left eyes (Fig. 12), but after the blip torsion was removed, the torsional movements were approximately the same in both eyes. Figure 13 illustrates this for a representative *subject CL*. Saccades were made to targets at four different eccentricities to the right. Torsion in the right eye (—) was approximately the same as that in the left eye (---), after correcting for the blip torsion. In the CCW condition, the torsion in the right eye was slightly bigger than that in the left eye in this subject, but this pattern was not consistently observed and in fact, reversed in one subject (*NH*). The overall mean value for the cyclovergence component of the torsional correction across all subjects was only  $0.15 \pm 0.17^\circ$  for horizontal saccades. Similarly, intrasaccadic torsional corrective movements were largely conjugate for vertical saccades; after correcting for the blip-torsion in all subjects, the mean cyclovergence across all subjects was only  $0.17 \pm 0.14^\circ$ . The amount of cyclovergence was not significantly different between horizontal and vertical saccades.

#### Coupling of torsion to vertical but not to horizontal saccades

When oblique saccades are made in which the horizontal or vertical component is larger, there is often "stretching" of the smaller of the two components (be it vertical or horizontal) with a corresponding increase in duration and decrease in peak velocity. We wondered whether a similar phenomenon could



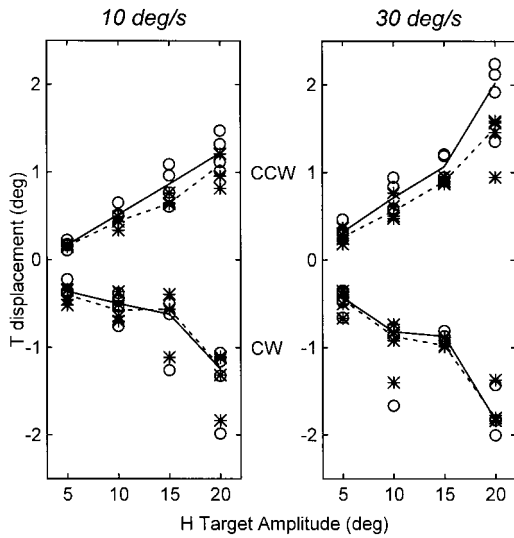


FIG. 13. Conjugacy of torsional movements in *subject CL*. Each mark represents the torsional component of the displacement vector of the blip-subtracted L-saccades. Torsion in the right eye (○) and in the left eye (\*) are grouped by OKN disk speed (10 or 30°/s) and by the direction of disk rotation, CCW (top in each panel) or CW (bottom). The solid and dotted lines connect median torsional displacements for the right and left eyes, respectively. Note that the magnitude of torsion displacement is similar in both eyes.

be observed with the torsional component of horizontal and of vertical L-saccades. The relationship of the peak velocity of the blip-subtracted intrasaccadic torsion to saccade amplitude appeared to be different for horizontal and for vertical saccades, although there was intersubject variability (Fig. 14). For horizontal saccades, peak torsional velocity of blip-subtracted L-saccades tended to increase with the amplitude of horizontal saccades. On the other hand, for vertical saccades, either the peak torsional velocity tended to decrease with the amplitude of vertical saccades, or there was little relationship between peak torsional velocity and saccade amplitude (Fig. 14 and Table 2). The difference in the slopes of the regression lines

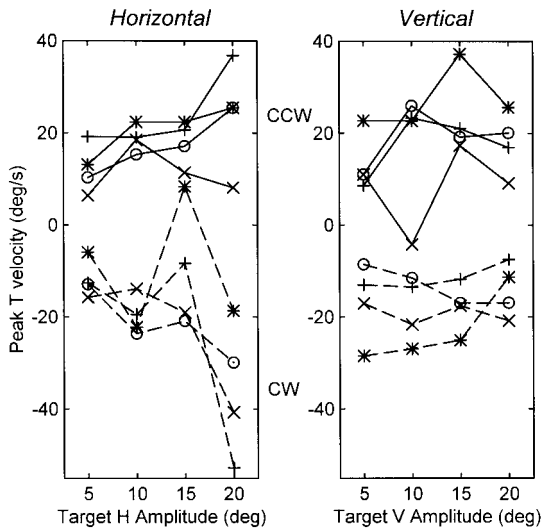


FIG. 14. Peak velocity of blip-subtracted torsion of L-saccades for all 4 subjects, during horizontal (*left panel*) and vertical (*right panel*) saccades. Each symbol represents the mean of peak velocity for each target condition for each subject. In all cases, the OKN disk was rotating at 30°/s. Lines drawn through data points indicate the mean values for each of 4 subjects; *CL* (○), *DZ* (\*), *MH* (+), and *NH* (×). See text for explanation.

relating the peak torsional velocity to saccade amplitude for horizontal and vertical saccades was prominent in the CW stimulus condition, and observed in both eyes. For example, the overall slope for horizontal saccades in the CW condition was  $-1.22$ , indicating that the peak torsional velocity increases with horizontal target amplitude (the corrective torsional movement is negative in the CW condition). The slope for vertical saccades was  $0.17$ , suggesting that the peak torsional velocity tended to decrease, if anything. For CCW conditions, the slopes did not actually reverse sign, but the slope was nonetheless less for vertical saccades ( $0.41$  vs.  $0.68$ ).

To further determine whether the torsional component was coupled to the vertical, but not to the horizontal component, the torsional velocity of blip-subtracted L-saccades was plotted against the horizontal or vertical component of angular velocity. In all four subjects, the time that peak torsional velocity was reached occurred later as vertical saccade amplitude increased and thus the ratio of torsional velocity to vertical velocity at the time of the peak torsional velocity (“T/V ratio”) systematically decreased (Fig. 15A). This result is compatible with the idea that torsion is coupled to the vertical system. No such systematic relationship was found between the torsional and horizontal components of angular velocity (Fig. 15B). We emphasize, however, that although the duration of vertical saccades was greater than those of horizontal saccades of matching amplitudes, there were no consistent increases in duration for either horizontal or vertical L-saccades compared with D-saccades.

Horizontal L-saccades were often dysmetric, missing the visual target because of a directional error in saccade accuracy. Figure 16 shows trajectories of primary saccades made toward a target  $15^\circ$  to the right, taken from a representative subject (*CL*). When a CCW torsional offset was induced, the endpoints of the primary saccades contained an error with an unwanted upward component. This error in vertical direction was reduced with subsequent corrective saccades (arrows in Fig. 17). Figure 18 shows a quantitative summary of saccade error for both horizontal and vertical saccades for all subjects. To summarize the size and direction of saccade error, median endpoints of D-saccades and L-saccades (asterisks in Fig. 16) were calculated. H and V errors were defined as the difference between these two median points in the horizontal and vertical dimensions, respectively. Saccade errors were greater with

TABLE 2. Slope of regression lines relating the peak torsional velocity to the target amplitude shown in Fig. 14

Subject	Symbol	Horizontal		Vertical	
		CW	CCW	CW	CCW
<i>CL</i>	○	-0.96	0.94	-0.61	0.41
<i>DZ</i>	*	-0.15	0.74	1.06	0.46
<i>MH</i>	+	-2.18	1.09	0.36	0.45
<i>NH</i>	×	-1.60	-0.04	-0.14	0.32
Total		-1.22 (-0.60)	0.68 (0.33)	0.17 (0.08)	0.41 (0.16)

Each entry is the slope of the regression line through the means of the peak torsional velocity of blip-subtracted L-saccades of the right eye in each target condition when the optokinetic disk was rotating at 30°/s. This, basically, is a numerical recapitulation of the data shown in Fig. 14. Total slopes are mean of all subjects, and numbers in parentheses are those for the left eye.

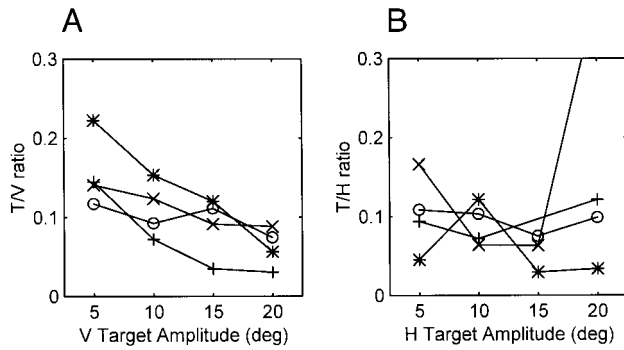


FIG. 15. Possible coupling between the torsional and vertical components. *A*: ratio of blip-subtracted torsional velocity to vertical velocity at the time of the peak torsional velocity ("T/V ratio") is plotted as a function of the vertical amplitude of the target. The OKN disk was rotating 30°/s CW. Each point represents the T/V ratio of the median trace of L-saccades after the median of D-saccades of the same block was subtracted, for *CL* (○), *DZ* (\*), *MH* (+), and *NH* (×). *B*: similar plots for horizontal saccades. The data point for 15° of subject *MH* (+) was far outlying, and data for 10 and 20° are connected. The OKN disk was rotating at 30°/s CW. Note the systematic reduction of T/V ratio with an increase of target vertical amplitude and thus saccade amplitude.

larger amplitude saccades, and accordingly in Fig. 18, saccades toward targets at 15 and 20° to the right (Horizontal) were combined, and likewise for 15 and 20° up (Vertical). As shown in Fig. 16, horizontal saccades with the CCW torsional offset condition ended higher than D-saccades, thus containing positive V errors (filled symbols of Fig. 18, Horizontal). Similarly horizontal saccades with the CW torsional offset ended lower than D-saccades, thus containing negative V errors (open symbols of Fig. 18, Horizontal). For vertical saccades, however, no consistent error in saccade end position with respect to D-saccades was found (Fig. 18, Vertical). Person's  $\chi^2$  test was performed to determine whether the polarity of saccade error

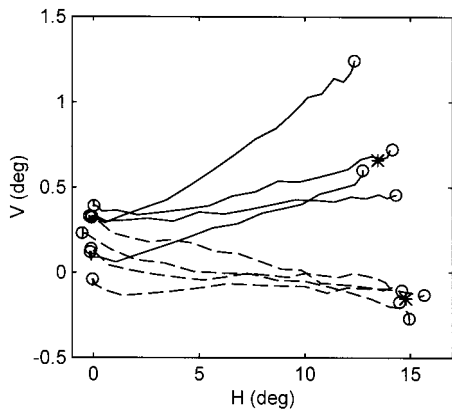


FIG. 16. Error in the end position of L-saccades made toward a target at 15° to the right for subject *CL*. Here rightward is plotted to the right and upward, up. The start and end positions of each primary saccade are indicated by circles. Saccade start points are near H 0 and V 0 degrees. Dashed trajectories are shown for 4 saccades made in the dark (D-saccades). The median end position is indicated by an asterisk. Solid lines are 4 saccades within the same block made to the same target with a torsional offset induced by the disk rotating at 30°/s in the CCW direction. The endpoints of these saccades contained an unwanted upward deflection that was then reduced by subsequent corrective saccades (not shown here but see Fig. 17). The median end position is indicated by another asterisk. Hausteijn (1989) suggested a correction to express gaze direction from rotation vectors, and for the purpose of this and following figures, the correction was made. The median end positions plotted in this figure with and without the correction differed  $<0.02^\circ$  in the horizontal component and approximately  $0.12^\circ$  in the vertical component for both D- and L-saccades.

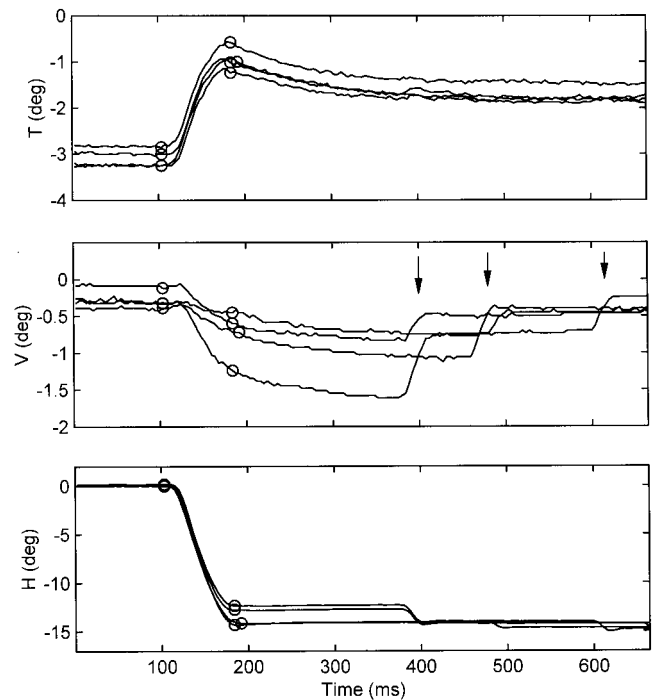


FIG. 17. Saccade error and its correction. The torsional (*top*), vertical (*middle*), and horizontal (*bottom*) traces of 4 L-saccades. Onsets and offsets of primary saccades as determined from horizontal traces are marked with circles, and onsets are aligned at 100 ms. The primary saccades between 2 circles are also shown in Fig. 16. Note that counterclockwise (intorsion in this right eye), upward and rightward rotations are negative. Arrows in the *middle panel* mark corrective saccades compensating for the vertical directional errors made during the primary saccades between circles, in response to the horizontal target displacement.

and the direction of torsional offset (CW or CCW) were statistically independent. For horizontal saccades, they were not statistically independent ( $\chi^2 = 21.13, P < 0.001$ ), whereas for vertical saccades, they were independent ( $\chi^2 = 3.77, P >$

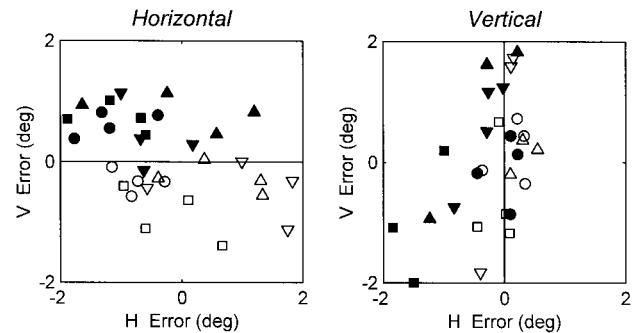


FIG. 18. Errors in saccade end position. *Left*: each symbol represents the median saccade error of each block when the target was either 15 or 20° to the right and the disk was rotating at either 10 or 30°/s CW (open) or CCW (filled). Positive values are right and up. The horizontal line represents zero vertical error. Data from different subjects are marked with different symbols: circles (*CL*), squares (*DZ*), triangles (*MH*), and inverted triangles (*NH*). For CCW rotation (filled), saccades show a positive vertical error indicating that they end with an inappropriate up component, whereas for CW rotation (open), saccades end with an inappropriate down component. *Right*: similar plots for errors of vertical saccades, to 15 and 20° upward with the disk rotating at 10 and 30°/s. The vertical line indicates zero horizontal error in saccade end position. Unlike horizontal saccades, vertical saccades showed no consistent pattern of error depending on stimulus condition. Three outlying data points with vertical error larger than 2, an open triangle with positive H error, an open inverted triangle and a filled square with negative H errors, were eliminated.

0.05). Thus the accuracy of horizontal and vertical saccades is differentially affected when a torsional error is introduced.

## DISCUSSION

A fundamental question in ocular motor physiology is how Donders' and Listing's laws are maintained. Current hypotheses include both peripheral (mechanical) explanations (Demer et al. 1997, 2000; Quaia and Optican 1998; Raphan 1998; Schnabolk and Raphan 1994) and central (neurally encoded) explanations (Crawford and Guitton 1997; Klier and Crawford 1998; Tweed et al. 1998; Van Opstal et al. 1996). Here we addressed a specific aspect of this issue by examining how visually induced torsional offsets, which temporarily take the eyes out of Listing's plane, are corrected. The main conclusion is that a neurally encoded central command is responsible for correcting such torsional errors, and that the correction takes place in association with the occurrence of horizontal or vertical saccades, implying three-dimensional control of saccades. We will first discuss potential confounding factors that might argue against this interpretation.

### *Torsional "blips"*

Torsional blips, which transiently take the eye out of Listing's plane during normal horizontal and vertical saccades, must be considered to make an accurate interpretation of the nature of any torsional corrective movements during saccades. We believe our corrections for such blips were accurate since subtraction of the saccade-induced blip torsion from the total intrasaccadic torsion of L-saccades (saccades with induced torsional offset) produced *symmetrical* torsional corrections. Furthermore the corrections were equally accurate whether the direction of the torsional offset was the same or opposite to the blip torsion.

### *Active versus passive control of torsion*

A second key question is whether or not the intrasaccadic torsional corrections are simply generated passively by the mechanical characteristics of the ocular motor plant. Seidman et al. (1995), based on the course of return of the eye to the resting position after mechanical displacements into extorsion and intorsion, reported that the return of the torsional position of the eye was asymmetric; the time constant of return from extorsion was 83 ms, whereas that from intorsion was 210 ms. In contrast, in our study the correction of the torsional offsets, after subtracting the torsional blip, was much faster than the return of the eye after a mechanical displacement. The time constant of the correction for the stimulus-induced torsion was approximately 20 ms (Fig. 5), and we found no asymmetry in the time course of these corrective torsional movements. This is strong evidence that the torsional error, i.e., the offset from the Listing's plane, is corrected by an active, neural, mechanism.

In a control experiment, we examined the return of the eye toward the Listing's plane following optokinetic stimulation. The time course of the return was  $>380$  ms, and much larger than the average values for the passive return from the mechanically displaced torsion. One might conclude that in this paradigm the slow "passive" return in the absence of a saccade during the control paradigm reflects the properties of the tor-

sional optokinetic system, or of the torsional velocity-to-position gaze-holding integrator. In either case, the slow decay of torsion would reflect the dissipation of "stored" activity, which had outlasted the time course of the passive orbital forces.

Finally, and perhaps most importantly, the main-sequence relationship between peak velocity and amplitude for the torsional corrections was comparable to that for the pure torsional quick phases that were elicited during roll optokinetic stimulation. This finding also argues strongly for a central mechanism underlying the correction of torsional errors during saccades.

### *Three-dimensional control of saccades and quick phases*

Based on the dependence of the torsional displacement during spontaneous saccadic eye movements on the initial torsional position, Van Opstal et al. (1996) concluded that errors in torsional position are monitored and corrected during the subsequent saccade, and that the correction is driven by a central three-dimensional command. Crawford and Guitton (1997) developed a model for the three-dimensional control of saccades and predicted one of the main results of our experiments: the active correction of torsion toward Listing's plane during horizontal and vertical saccades. Thus our results also support the idea that torsional error is monitored and actively corrected by a central three-dimensional neural control mechanism, rather than by a passive plant property. Put in another way, central saccade circuits can encode three-dimensional eye movement commands when there is a need to restore eye positions back to Listing's plane. This will ensure correct torsional eye orientation during fixation. Our findings and this interpretation are consonant with what has been reported in monkeys when their eyes were artificially moved out of Listing's plane by electrical stimulation in the caudal aspect of the nucleus reticularis tegmenti pointis (cNRTP) (Van Opstal et al. 1996). As in our experiments, the torsional error was corrected in association with the next saccade. One important caveat should be kept in mind, however. Both our results and those of Van Opstal et al. (1996) do not exclude a role for orbital muscle pulleys in the mediation of centrally generated command in the control of eye torsion, since orbital muscle pulleys seem to have a neural innervation (Demer et al. 2000).

### *Anatomic substrate for the control of ocular torsion*

One important question is which structures within the brain mediate these three-dimensional control mechanisms. Since lesions in the cNRTP impair this torsional correction mechanism (Van Opstal et al. 1996), it may be that the cerebellum, which receives projections from the cNRTP, plays a role in correcting torsional deviations from Listing's plane, and that cerebellar lesions might lead to a torsional dysmetria in which the eyes are not properly brought to Listing's plane in association with horizontal or vertical saccades. The abnormality of saccade-associated torsion described by Helmchen et al. (1997) and by Morrow and Sharpe (1988) in patients with lesions in the dorsal lateral medulla and cerebellum support this idea. There is additional evidence for a role for the cerebellum in the control of torsional eye position and Listing's plane. Patients with diffuse cerebellar degenerations also show abnormalities of the control of torsional eye position; they have abnormal

torsional drift that changes with orbital position (Straumann et al. 2000).

#### *Coupling of torsional corrections and vertical saccades*

Another important result in our study is the apparent difference in the coupling between torsional and vertical, and between torsional and horizontal saccades. Whereas for horizontal saccades, peak torsional velocity increased with the amplitude of horizontal saccades, this was not the case for peak torsional velocity and the amplitude of vertical saccades. Furthermore, the time when peak torsional velocity was reached was delayed as the amplitude of vertical saccades increased but there was no such relationship between torsional peak velocity and the amplitude of horizontal saccades. Thus the patterns of coupling between the dynamic properties of torsional saccades and of horizontal or vertical saccades were different.

Systematic errors in saccade *accuracy* were also seen when torsional corrections were coupled with horizontal but not with vertical saccades. Currently no saccade model accounts for this differential effect. Crawford and Guitton (1997) considered saccade accuracy to test properties of their three-dimensional models for generating kinematically correct saccades and pointed out that errors in saccade accuracy might occur with torsional offsets unless there were specific adjustments in premotor commands for saccades depending on three-dimensional eye position. Furthermore, the adjustments in their model had to be at a specific location (“upstream”) relative to a “Listing’s law operator.” They did not, however, predict a different pattern of dysmetria depending on whether the saccade was vertical or horizontal nor was one found when Klier and Crawford (1998) looked for directional errors in normal subjects with a torsional offset (counterroll) induced by head tilt. They did find, however, small directional errors but with a general trend for the errors to be in the opposite direction as the counterroll of the eyes, which is the opposite to our findings for horizontal saccades. For example, with CCW torsional offset, more of a down component was observed for rightward saccades (Figs. 10B and 11C of Klier and Crawford 1998), whereas in our study more of an up component was found (Figs. 16 and 18). In their paradigm the torsional offset of the eyes was produced by a head tilt, and saccades were made while the head tilt was maintained, and thus were basically two-dimensional and within Listing’s plane. Thus in their paradigm, although an initial torsional offset existed when saccades started, the torsional offset was not and did not have to be corrected. In our paradigm, in contrast, the torsional offset occurred without any actual rotation of the head in space, and in that sense did not serve the same purpose as a natural counterroll. Hence subsequent saccades incorporated a torsional correction to bring the eyes back toward Listing’s plane.

To epitomize, our results suggest the presence of coupling between the torsional and vertical, but not between the torsional and horizontal systems, both with respect to saccade accuracy as well as to saccade dynamic properties. The errors in saccade accuracy associated with horizontal but not vertical saccades suggest that the vertical-torsional saccade-generating circuits in the rostral interstitial nucleus of medial longitudinal fasciculus (riMLF) may receive a desired eye orientation signal that takes into account the torsional error, while the horizontal saccade-generating circuits in the pons do not. The correction

of torsional offsets, however, takes place with saccades of either direction, implying a separate mechanism for programming a correction to keep the eyes in Listing’s plane. With respect to the dynamic aspects of coupling of torsion during saccades, it seems possible that the selective coupling for vertical saccades reflects the common neural substrate in the riMLF for generating premotor saccade commands for both torsional and vertical rapid eye movements. Finally, some coupling of torsion to vertical motion might also occur in the ocular motor periphery because of sharing of muscles for torsion and vertical rotations of the globe. But the active, centrally commanded nature of the torsional correction is still suggested by the time course of the torsional correction, which was quite rapid during horizontal as well as vertical saccades. It should be pointed out, however, that the coupling between torsional and vertical components is not exactly like the one between horizontal and vertical components showing so-called component stretching, since there was no consistent increase in duration of horizontal or vertical L-saccades compared with D-saccades.

#### *Implications for three-dimensional saccade generation models*

The torsional error was corrected synchronously with the horizontal or vertical error, but its correction during the primary saccade was incomplete, leaving a residual torsional error to be corrected by other mechanisms with longer time constants (Fig. 8A, and also see for an individual example, the 1st and 2nd figures in the *right panel* of Fig. 4). The ratio of corrected torsion to the initial torsional offset was linearly related to horizontal or vertical saccade amplitude (Fig. 8B), indicating that the torsional correction is yoked to the horizontal or vertical correction. Thus although the saccade itself is three-dimensional, saccade duration is determined by the error in the horizontal or vertical, but not in the torsional component. Robinson (1975) was the first to propose the local feedback hypothesis controlling saccade generation, and numerous modifications of the original model (Gancarz and Grossberg 1998; Jürgens et al. 1981; Quaia and Optican 1998; Scudder 1988, to list only a few) have appeared. In these models, saccade amplitude and duration are determined by signals of desired and current eye position, orientation, or displacement provided by local feedback. The yoked torsional correction suggests that the local feedback loops that control saccade *amplitude* and *duration* are two-dimensional in nature, i.e., feedback for horizontal and vertical orientations only, and that Donder’s and Listing’s laws are implemented downstream from local feedback loops.

We thank A. Lasker for providing technical expertise in building and operating the stimuli and D. Roberts for computer programming and help with data collection.

This research was supported by the Korea Research Foundation (98-001-C01153), the Korea Ministry of Science and Technology under the Brain Science Research Program, National Eye Institute Grant RO1-EY01849, the Swiss National Science Foundation (3231-051938.97/3200-052187.97), and the Betty and David Koetser Foundation for Brain Research.

Address for reprint requests: C. Lee, Dept. of Psychology, Seoul National University, Kwanak, Seoul 151-742, Korea.

Received 2 August 1999; accepted in final form 8 February 2000.

## REFERENCES

- BALLIET R AND NAKAYAMA K. Training of voluntary torsion. *Invest Ophthalmol Vis Sci* 17: 303–314, 1978.
- BRUNO P AND VAN DEN BERG AV. Torsion during saccades between tertiary positions. *Exp Brain Res* 117: 251–265, 1997.
- COLLEWIJN H, VAN DER STEEN J, FERMAN L, AND JANSEN TC. Human ocular counterroll: assessment of static and dynamic properties from electromagnetic scleral coil recordings. *Exp Brain Res* 59: 185–196, 1985.
- CRAWFORD JD AND GUITTON D. Visuomotor transformations required for accurate and kinematically correct saccades. *J Neurophysiol* 78: 1447–1467, 1997.
- DEMER JL, OH SY, AND POUKENS V. Evidence for active control of rectus extraocular muscle pulleys. *Invest Ophthalmol Vis Sci*. In press.
- DEMER JL, POUKENS V, MILLER JM, AND MICEVYCH P. Innervation of extraocular pulley smooth muscle in monkeys and humans. *Invest Ophthalmol Vis Sci* 38: 1774–1785, 1997.
- DONDERS FC. Beiträge zur Lehre von den Bewegungen des menschlichen Auges. *Holländische Beiträge zu den Anatomischen und Physiologischen Wissenschaften* 1: 105–145, 1848.
- GANCARZ G AND GROSSBERG S. A neural model of the saccade generator in the reticular formation. *Neural Networks* 11: 1159–1174, 1998.
- HAUSTEIN W. Considerations on Listing's Law and the primary position by means of a matrix description of eye position control. *Biol Cybern* 60: 411–420, 1989.
- HELMCHEN C, GLASAUER S, AND BUTTNER U. Pathological torsional eye deviation during voluntary saccades: a violation of Listing's law. *J Neurol Neurosurg Psychiatry* 62: 253–260, 1997.
- V HELMHOLTZ H. *Handbuch der Physiologischen Optik*. Hamburg und Leipzig: L Voss, 1867.
- HEPP K. On Listing's law. *Commun Math Physics* 132: 285–292, 1990.
- HEPP K, VAN OPSTAL AJ, SUZUKI Y, STRAUMANN D, HESS BJM, AND HENN V. Listing's law: visual, motor or visuomotor? In: *Three-Dimensional Kinematics of Eye, Head and Limb Movements*, edited by Fetter M, Haslwanter T, Misslisch H, and Tweed D. Amsterdam: Harwood Academic Publishers, 1997.
- JÜRGENS R, BECKER W, AND KORNUBER H. Natural and drug induced variations of velocity and duration of human saccadic eye movements: evidence for a control of the neural pulse generator by local feedback. *Biol Cybern* 39: 87–96, 1981.
- KLIER EM AND CRAWFORD JD. Human oculomotor system accounts for three-dimensional eye orientation in the visual-motor transformation for saccades. *J Neurophysiol* 80: 2274–2294, 1998.
- MELIS BJ AND VAN GISBERGEN JA. Analysis of saccadic short-term plasticity in three dimensions. *Vision Res* 35: 3423–3437, 1995.
- MORROW MJ AND SHARPE JA. Torsional nystagmus in the lateral medullary syndrome. *Ann Neurol* 24: 390–398, 1988.
- QUAIA C AND OPTICAN LM. Commutative saccadic generator is sufficient to control a 3-d ocular plant with pulleys. *J Neurophysiol* 79: 3197–3215, 1998.
- RAPHAN T. Modeling control of eye orientation in three dimensions: role of muscle pulleys in determining saccade trajectory. *J Neurophysiol* 79: 2653–2667, 1998.
- REMMEL RS. An inexpensive eye movement monitor using the scleral search coil technique. *IEEE Trans Biomed Eng* 31: 388–390, 1984.
- ROBINSON DA. Oculomotor control signals. In: *Basic Mechanisms of Ocular Motility and Their Clinical Implications*, edited by Bach-y-Rita P and Lennestrand G. Oxford, UK: Pergamon, 1975, p. 337–374.
- SCHNABOLK C AND RAPHAN T. Modeling three-dimensional velocity-to-position transformation in oculomotor control. *J Neurophysiol* 71: 623–638, 1994.
- SCUDDER CA. A new local feedback model of the saccadic burst generator. *J Neurophysiol* 59: 1455–1475, 1988.
- SEIDMAN SH, LEIGH RJ, TOMSAK RL, GRANT MP, AND DELL'OSSO LF. Dynamic properties of the human vestibulo-ocular reflex during head rotations in roll. *Vision Res* 35: 679–689, 1995.
- STRAUMANN D, ZEE DS, AND SOLOMON D. Three-dimensional kinematics of ocular drift in humans with cerebellar atrophy. *J Neurophysiol* 83: 1125–1140, 2000.
- STRAUMANN D, ZEE DS, SOLOMON D, AND KRAMER PD. Validity of Listing's law during fixations, saccades, smooth pursuit eye movements, and blinks. *Exp Brain Res* 112: 135–146, 1996.
- STRAUMANN D, ZEE DS, SOLOMON D, LASKER AG, AND ROBERTS DC. Transient torsion during and after saccades. *Vision Res* 35: 3321–3334, 1995.
- SUZUKI Y, STRAUMANN D, HESS BJM, AND HENN V. Changes of Listing's plane under physiological and pathological conditions. In: *Information Processing Underlying Gaze Control*, edited by Delgado-Garcia JM, Godaux E, and Vidal PP. Oxford, UK: Pergamon, 1994, p. 75–86.
- TWEED D, HASLWANTER T, AND FETTER M. Optimizing gaze control in three dimensions. *Science* 281: 1363–1366, 1998.
- TWEED D, MISLISCH H, AND FETTER M. Testing models of the oculomotor velocity-to-position transformation. *J Neurophysiol* 72: 1425–1429, 1994.
- VAN OPSTAL AJ. Representation of eye position in three dimensions. In: *Multisensory Control of Movement*, edited by Berthoz A, Gielen C, Henn V, Hoffmann KP, Imbert M, Lacquaniti F, Roucoux A, Viviani P, and Van Gisbergen J. Oxford, UK: Oxford Univ. Press, 1993.
- VAN OPSTAL AJ, HEPP K, SUZUKI Y, AND HENN V. Role of monkey nucleus reticularis tegmenti pontis in the stabilization of Listing's plane. *J Neurosci* 16: 7284–7296, 1996.